Using Perturbation Force Analysis for the Design of a Levitron© : an Application of Magnetic Levitation

Z. De Grève*,1,2, C. Versèle[1], and J. Lobry[1]
[1]Faculty of Engineering, Mons, Belgium, [2]Belgian Fund for Research, F.R.S./FNRS, Research Fellow
*Bd Dolez, 31, BE-7000 Mons, zacharie.degreve@fpms.ac.be

Abstract: The Levitron© offers an interesting demonstration of natural magnetic levitation using permanent magnets. It is composed by a small magnetized top and a circular magnetized base with a hole on its centre. The top is placed in an area where magnetic field configuration and gyroscopic torques allow the existence of a locus of stable equilibrium. In this paper, we intend to dimension and realize a Levitron© in laboratory, starting from second-hand components. To that end, these components are first identified (in terms of volume magnetization) by comparing magnetic induction measurements to induction estimated through COMSOL finite element models. Then, a perturbation force analysis is performed to derive the locus of stable equilibrium. Stability is obtained when top axial and radial excursions are compensated by opposite perturbation forces. We compare three different methods for the estimation of forces in our application, two based on the virtual work theorem and one performing numerical integration of the classical expression of force between magnets. Results, after being compared with a simple analytical model available in litterature, are actually employed to create a Levitron© using identified components.

Keywords: magnetic levitation, magnetic force estimation, permanent magnets

1 Introduction

Even if common people are more familiar with the attractive aspect of magnetic forces (lifting electromagnets, etc.), magnetic repulsion forces require our interest, for the numerous possibilities they offer. Indeed, in a correctly designed system, gravity can be overcome without the necessity of a material structure to be present. We thus understand the reason why engineers are particularly concerned with the magnetic levitation phenomenon these years (*e.g.* magnetic levitation trains, such as Japanese *Maglev* and German *Transrapid*).

The impossibility to maintain a magnetized body in stable levitation using *static* fields has been proven in 1842 by Earnshaw[1]. Thus, to make magnetic levitation viable, several possibilities have been investigated. Numerous applications, such as Japanese *Maglev*, are based on superconductor levitation. Indeed, superconductors can be considered as perfect diamegnetic bodies ($\mu_r \simeq 0$), which have the property to repel applied magnetic fields, and are not embraced in Earnshaw theory. Other solutions, which include a dynamical aspect into the system to avoid Earnshaw's theorem limitations, are also currently available. Servomechanisms are for instance emlployed to assure magnetic levitation : the German *Transrapid* motions are continuously adjusted through a feedback loop which regulates the current flowing in electromagnet windings. Levitation due to induced currents is also feasible : an iron plate placed in an alternating magnetic field can be lifted by the Laplace forces acting on eddy current loops. Finally, we speak about gyroscopic levitation when a rotating magnet is maintained in stable levitation by gyroscopic effects. The Levitron©, that we intend to study during this paper, belongs to this last category.

A Levitron© is composed by a top (a non-magnetic spindle inserted in a flat, or

[1] Earnshaw theorem precludes the existence of potential extrema for a static configuration of electric (or magnetic) particles, thus forbidding stable equilibrium.

toroïdally shaped, permanent magnet) and by a magnetized base with a circular hole on its centre. An unmagnetized guide is also required in order to bring the rotating top into the locus of stable equilibrium (figure 1). Gyroscopic torques acting on the spinning top maintain it in a nearly vertical alignment, so as to prevent it being flipped over. Therefore, strong dipole-dipole repulsion forces can suspend the top against gravity, in a locus of stable equilibrium.

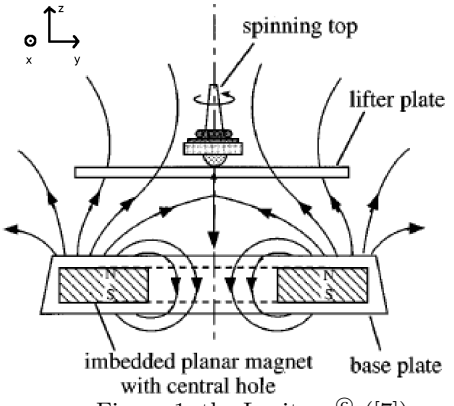

Figure 1: the Levitron© ([7])

This work aims to dimension and realize a Levitron© in laboratory, using second hand components such as ferrite permanent magnets from old speakers and *Ne-Fe-B* magnets. To do so, magnetic component parameters are first identified (volume magnetization M). This is done by comparing magnetic induction measurements along magnet z axis, obtained via a Hall effect gaussmeter, and the induction estimated through COMSOL Multiphysics models (section 3). Then, a perturbation force analysis is applied to derive the locus of stable equilibrium : stability is obtained when top radial or axial excursions are compensated by opposite perturbation forces (section 4). Top mass is thereafter estimated by opposing magnetic force exerted on it to gravity. Three methods will be compared for the computation of magnetic forces, two based on virtual work theory and one performing the numerical integration of classical expression of forces between permanent magnets (subsection 4.2). Finally, after being compared with a simple analytical model available in litterature ([7] and [8]), results will be employed to create a Levitron© using identified components.

It is important to note that this paper focuses on magnetic aspects only, in order to derive conditions assuring stable levitation. Mechanical aspects are not adressed in our study : the impact of top rotation speed against stability is for instance not discussed. However, the authors are convinced that their approach can be used as a base for the comprehension of the complex phenomenolgy of the Levitron©, and recommend [5] and [6] for more detailed models.

2 Numerical model

We employed second-order Lagrangian tetrahedron to discretize the problem geometry. Due to the absence of real currents, the total magnetic scalar potential ψ was approximated on the nodal elements, leading to the following local form :

$$\Omega \ : \ -\mu_0\vec{\nabla}(\vec{\nabla}\psi) + \mu_0\vec{\nabla}\vec{M} = 0 \qquad (1)$$

Magnets constitutive law was the following :

$$\vec{B} = \mu_0(\vec{M} + \vec{H}), \qquad (2)$$

where $\vec{B}$ is the magnetic induction, $\vec{H}$ the magnetic field, and $\vec{M}$ the volume magnetization, which is constant (rigid permanent magnets) and uniformly z oriented.

The weak form was derived from equation 1 and the problem solved for ψ using COMSOL Multiphysics application mode *AC/DC module - Magnetostatics - No Currents*. Radial excursions of the top, as explained in 4.1, forced us to use a $3D$ cartesian model rather than a more simple axisymmetric $2D$ one. A Conjugate Gradient resolution procedure showed fast convergence towards the solution.

We imposed magnetic insulation along system boundaries ($\vec{B}\vec{n} = 0$), which is equivalent to set :

$$\Gamma \ : \ \frac{\partial\psi}{\partial n} = 0 \qquad (3)$$

Magnetic field and its derivatives were obtained *a posteriori* using the following classical relation. If $\hat{\psi}$ represent the approximated value of scalar magnetic potential and N_j the basis functions at node j, we have, for second order tetraedrons :

$$H_i = \sum_{j=1}^{10} \frac{\partial N_j(x,y,z)}{\partial i} \hat{\psi_j} \quad i = x, y, z \quad (4)$$

Note that built-in COMSOL functions should have been used for the same purpose, but multiple calls to *postinterp* routine for instance would have been too much time consuming.

3 Magnetic component identification

As no information is *a priori* available for ferrite and *Ne-Fe-B* magnets, magnetic models need first to be derived. To that end, magnetic induction measurements along magnets z axis, obtained using a Hall effect gaussmeter (figure 2), are compared with induction from COMSOL Multiphysics models.

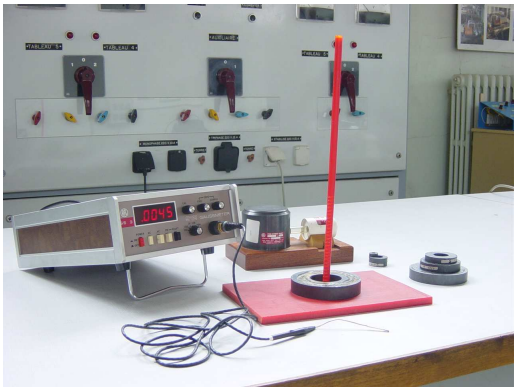

Figure 2: Our measurment station, model 912 gaussmeter (*RFL Industries Inc.*)

An estimator, the SNSE (for *Sum of Normalized Squared Errors*), defined as follows, is computed to account for the curves adjustment quality :

$$SNSE = \sum_{i=1}^{n} \left(\frac{H_{i,mes} - H_{i,sim}}{H_{i,mes}}\right)^2 \quad (5)$$

Volume magnetization M is tuned in order to minimize the SNSE. Figure 3 compares two curves, the measured and the simulated one, for a particular magnet, and table 1 summarizes identification results. The B_i magnets are candidate for the Levitron© base construction whereas the T_i ones for the top.

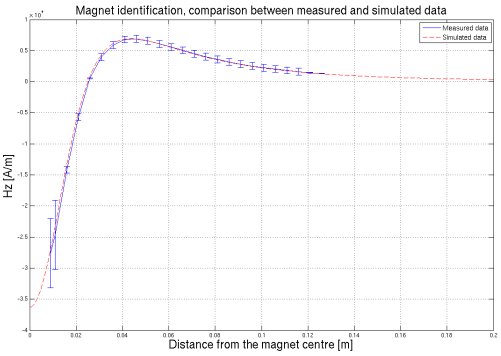

Figure 3: Magnet identification: magnetic field along z axis versus distance from magnet centre

Magnet code	M_z***[A/m]***	***SNSE***
B_1	183000	0.078
B_2	172500	0.024
B_3	227500	0.024
B_4	250000	0.076
B_5	192000	0.038
T_1	190000	0.219
T_2	260000	0.021
T_3	765000	0.1

Table 1: Magnets volume magnetization. All magnets are in ferrite, except T_3 which is in *Ne-Fe-B*

4 Stability analysis

4.1 Method

For stable equilibrium to exist, small displacements of the top in any direction should be compensated by opposite forces, which would replace it in its previous position. In other words, force field lines should all point inwards, towards the equilibrium position, which means that the divegence of the force field should be negative.

However, Earnshaw's theorem states that such a situation cannot be encountered with static magnetic fields. In the Levitron©, the spinning top acts as a gyroscop, preventing its magnetic field to align itself in the same direction as that of the base. This fliping phenomenon, combined with top precession and nutation motions, allow the existence of a stable equilibrium area, where gravitation, magnetic and gyroscopic forces are compensated.

In our approach, based on [7], these two motions (precession and nutation) are ignored (orientational stability is considered as given), while assumptions are made about the top orientation during excursions around equilibrium position. More sophisticated models, which account for the complex dynamic of the Levitron©, are available in litterature ([5], [6]).

Two models ([7]) are investigated in this work. In the first, we consider that the top is spinning so rapidly that gyroscopic action maintains its magnetic moment perfectly aligned with z axis, irrespective of radial or axial excursions :

$$\vec{M} = M_z \vec{u}_z \tag{6}$$

Magnetization norm is supposed constant (rigid permanent magnets). The second model assumes that the top remains parallel to the base magnetic field during radial or axial excursions around equilibrium, phenomenon well observed in practice :

$$\vec{M} = M \frac{\vec{H}}{\left\| \vec{H} \right\|} \tag{7}$$

Geometry configuration during radial excursions forced us to adopt a tridimensional model instead of a simpler axisymmetric one, as it can be observed on figure 4.

Basing on these considerations, our approach for the design of the Levitron© will be the following. Axial (*i.e.* z oriented) and radial perturbation forces acting on the top will be computed from finite element simulations, for the two models (equations 6 and 7) and for different positions of the top along z axis. An equilibrium area will then be derived, considering the fact that stability is assured when perturbations are compensated (*i.e.* when perturbation force is opposite to displacement direction). Top mass will then be estimated by opposing magnetic force exerted on the top in stability area to gravity.

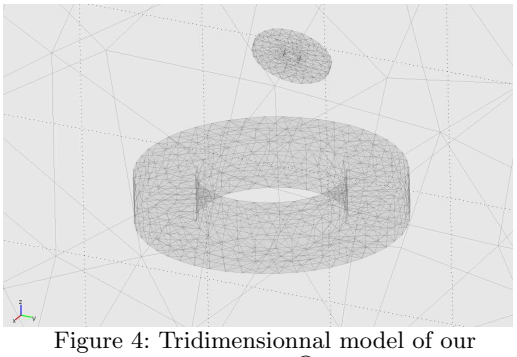

Figure 4: Tridimensionnal model of our Levitron©

4.2 Force computation

Three methods are investigated for the computation of perturbation forces from finite element simulations.

4.2.1 Numerical integration

The force exerted on a permanent magnet of magnetization $\vec{M}$ placed in an external magnetic field $\vec{H}$ (*i.e.* the base magnetic field) is given by ([2]) :

$$\vec{F} = \mu_0 \iiint_\Omega (\vec{M}\vec{\nabla})\vec{H} d\Omega, \tag{8}$$

and we have :

$$\begin{aligned} F_x &= \mu_0 \iiint_\Omega (M_x \frac{\partial H_x}{\partial x} + M_y \frac{\partial H_x}{\partial y} \\ &\qquad + M_z \frac{\partial H_x}{\partial z}) d\Omega \\ F_y &= \mu_0 \iiint_\Omega (M_x \frac{\partial H_y}{\partial x} + M_y \frac{\partial H_y}{\partial y} \\ &\qquad + M_z \frac{\partial H_y}{\partial z}) d\Omega \\ F_z &= \mu_0 \iiint_\Omega (M_x \frac{\partial H_z}{\partial x} + M_y \frac{\partial H_z}{\partial y} \\ &\qquad + M_z \frac{\partial H_z}{\partial z}) d\Omega \end{aligned} \tag{9}$$

Results from COMSOL simulations are transferred to MATLAB, where integrals in 9 are computed by performing a second order Gauss quadrature on the top subdomain. A MATLAB script is used to loop the procedure by continuously adjusting the system geometry, respecting equations 6 or 7, in order to derive the stability area for a given arrangement of available magnets. This method will be refered as NUMINT throughout this paper.

4.2.2 Coulomb Virtual Work method

In [3], the Virtual Work principle is employed to derive an expression for the magnetic force exerted on a rigid body, using the local jacobian derivative method. For a H oriented formulation, the magnetic co-energy is differentiated along the virtual displacement i, at constant scalar potential ψ, so as to obtain, for the force component along i axis :

$$F_i = \sum_e (\iiint_{V_e} -\vec{B} G^{-1} \frac{\partial G}{\partial i} \vec{H} dV_e + \iiint_{V_e} (\int_0^B B dH) \|G\|^{-1} \frac{\partial \|G\|}{\partial i} dV_e), \quad (10)$$

In equation 10, the sum extends to all elements e of the model, i stands for the direction of the virtual displacement and V_e represents the volume of the considered element. G is the jacobian matrix of the transformation which maps global coordinates to local element coordinates. All the elements belonging to the body are displaced all togeteher along i direction. Three categories of elements appear ; the fixed, the entirely movable and the distorted ones (figure 5). It can be shown that the co-energy is only modified in elements belonging to the third category, *i.e.* in air elements surrounding the movable body (top magnet), so that equation 10 is only computed on these elements. The amount of distorted elements can be arbitrarily fixed, but we chose the tetrahedron layer directly surrounding the top subdomain for simplicity. In that case, equation 10 becomes :

$$F_i = \sum_e (\iiint_{V_e} -\mu_0 \vec{H} G^{-1} \frac{\partial G}{\partial i} \vec{H} dV_e + \iiint_{V_e} \frac{\mu_0 \left\| \vec{H} \right\|^2}{2} \|G\|^{-1} \frac{\partial \|G\|}{\partial i} dV_e), \quad (11)$$

This procedure will be refered from now as Coulomb Virtual Work method (CVW).

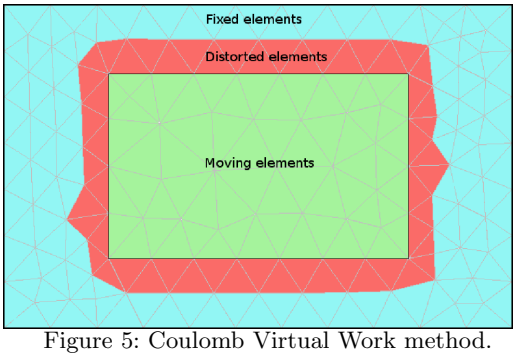

Figure 5: Coulomb Virtual Work method. Equation 11 is only computed on red elements

4.2.3 Local Virtual Work method

Unlike the CVW approach, where a set of nodes is simultaneously displaced, the local virtual work method (LVW) displaces a single node at a time ([4] and [1]). Only the co-energy (for a H oriented formulation) corresponding to the elements surrounding that node is modified during the virtual displacement. Thus, a local force, associated to the node, can be obtained by differentiating co-energy versus virtual displacement at constant scalar magnetic potential. De Medeiros *et.al.* derived the force expression in the case of rigid permanent magnets ([4]) :

$$F_{ik} = \frac{\mu_0}{2} \sum_{e_k} \iiint_{V_{e_k}} (-G^{-1} \frac{\partial G}{\partial i} \vec{H} (\vec{H} + \vec{M}) + (\vec{H} + \vec{M}) (-G^{-1} \frac{\partial G}{\partial i} \vec{H}) + (\vec{H} + \vec{M}) \|G\|^{-1} \frac{\partial \|G\|}{\partial i}) dV_{e_k} \quad (12)$$

Terms in equation 12 have the same signification than in equation 11. e_k stands for the elements surrounding node k, and global force is obtained by summing nodal forces on the nodes of the magnet.

5 Results and discussion

Numerous combinations of base candidate and top candidate magnets were possible and investigated, but only the results for the $B_5 - T_3$ configuration will be exposed, as it is the authors final choice, for practical reasons.

Figure 6 shows the evolution of z component of magnetic force acting on the top versus distance between the two magnets. We are only interested in the piece of curve with a negative slope, as it corresponds to an area where axial perturbations (*i.e* z oriented) are compensated. Forces obtained with the three methods (NUMINT, CVW and LVW) are represented. We observe that, considering the small value of total force in our configuration (around 0.2 N), CVW and LVW methods suffer from an exagerate sensibility to top position and meshing. For that reason, other following results will be exposed for the NUMINT method only.

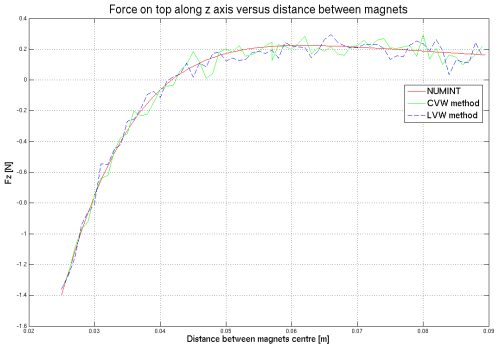

Figure 6: Force exerted on top, computed with the three methods NUMINT, CVW and LVW

In addition, to pretend to stability, radial perturbation forces have also to be compensated when the top performs radial excursions from z axis. Figure 7 accounts for these forces for the two models exposed in section 4.1, *i.e.* when $\vec{M}$ is rigidly z oriented or when it is directed along the base magnetic field. We observe that only the second model gives satisfactory results: we can find an area along z axis where axial and radial perturbation forces are simultaneously compensated, while it is not possible for the first model. This should not astonish us, since the second model is far more close from what we experimentally observe with a Levitron©. We obtain stable equilibrium between 62 mm and 68 mm, the lower limit corresponding to a top mass of 22.8 g and the upper to 22.3 g.

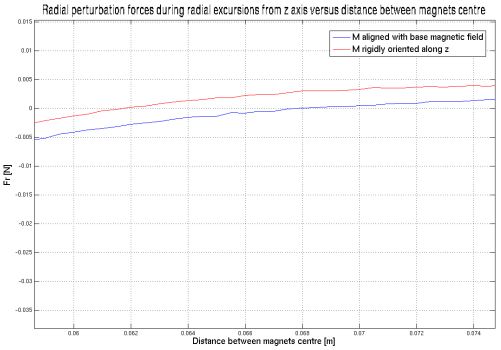

Figure 7: Radial perturbation forces, for the two M oriented models (NUMINT method)

These constatations have been employed to realize a Levitron© in laboratory. For the $B_5 - T_3$ configuration, stability have been observed between 62 mm and 68 mm (close to the simulated interval), for a top weighting between 25.9 g and 26.2 g. The gap between simulated and measured data can be explained by emphasizing measurement errors. Indeed, magnetic induction along z axis magnets have been measured with a gaussmeter, using a probe manipulated by hand, thus leading to inevitable approximations. When favorable conditions were gathered (base magnet carefully aligned with the vertical, etc.), stable magnetic levitation have been observed for $1min22s$ (figure 8).

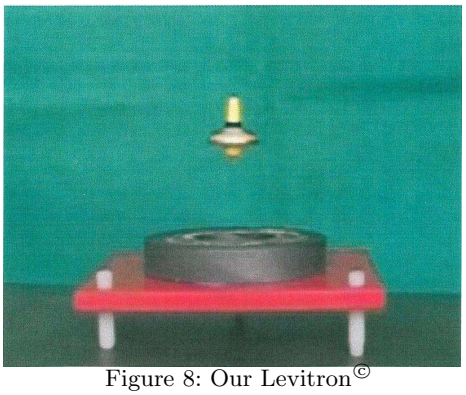

Figure 8: Our Levitron©

	Our approach	*Magnetic dipole approach[8]*	*Experimental results*
Stability Area *[mm]*	$62-68$	$61-66$	$62-68$
Top mass *[g]*	$22.3-22.8$	$19.7-20.3$	$25.9-26.2$

Table 2: Simulated and experimental results, for the $B_5 - T_3$ configuration (second M model)

Our results can be compared with a simple analytical model avalaible in litterature ([7]), in which the top is considered as a ponctual magnetic dipole. In [8], the authors computed a locus of stable equilibrium from 61 mm to 66 mm for the same magnet configuration, corresponding to top masses from 19.7 g to 20.3 g. All the results are summarized in table 2. We can observe that even if stability areas coincide for the two approaches, mass is closer from experimental measurements for the approach presented in this paper, which can be easily understood as magnetic forces are here computed by numerically integrating over the entire top, instead of considering simple dipole repulsion forces.

6 Conclusion

In this work, a finite element based procedure for the design of a Levitron©, using second-hand components, has been presented. After identifying magnets, a perturbation analysis has been performed to derive the locus of stable equilibrium, as well as top mass, for diverse magnet combinations. We saw that the top flipping motion was indispensable to assure stability: its magnetization vector indeed needs to adopt the same direction than the base magnetic field during radial excursions, without which axial and radial perturbations cannot be simultaneously compensated. We also showed that virtual work based methods for force computations, whereas giving satisfactory results in other general cases, suffer from an exagerate sensibility to top position and meshing, considering the small value of forces involved in our study. Thus, numerical integration of the classical expression of forces exerted on permanent magnets was successfully employed for our purpose.

Our results were compared with a simple analytical model, based on [7] and [8], in which the top is assimilated to a ponctual magnetic dipole, and with experimental measurements. We showed that stability areas were in good agreement with experience for the two models, whereas our estimation of the top mass was closer to reality, which can be easily explained as forces are estimated in our case by integrating over the entire top rather than considering simple dipole repulsion forces.

References

[1] Benhama A., Williamson A.C., and Reece A.B.J., *Virtual Work Approach to the Computation of Magnetic Force Distribution from Finite Element Field Solutions*, IEE Proc.-Electr.Power Appl. **147** (2000), no. 6, 437–442.

[2] Durand E., *Magnetostatique*, Masson et Cie, 1968.

[3] Coulomb J.L. and Meunier G., *Finite Element Implementation of Virtual Work Principle for Magnetic or Electric Force and Torque Computation*, IEEE Trans. on Mag. **20** (1984), no. 5, 1894–1896.

[4] De Medeiros L.H., Reyne G., Meunier G., and Yonnet J.P., *Distribution of Electromagnetic Force in Permanent Magnets*, IEEE Trans. on Mag. **34** (1998), no. 5, 3012–3015.

[5] Berry M.V., *The Levitron© : an Adiabatic Trap for Spins*, Proc. R. Soc. Lond. (1996), 1207–1220.

[6] Gans R.F., Jones T.B., and Washizu M., *Dynamics of the Levitron©*, J. Appl. Phys. **31** (1998), 671–679.

[7] Jones T.B., Washizu M., and Gans R., *Simple Theory for the Levitron©*, J. Appl. Phys. **82** (1997), no. 2, 883–888.

[8] De Greve Z., Versele C., and Lobry J., *Etude Theorique, Simulation et Realisation d'un Levitron© a l'aide du Logiciel de Calcul par Elements Finis COMSOL Multiphysics*, CETSIS Conf., 2008.